Supporting information

for

Nanoscale phosphorus-based agrochemicals enhance tomato and rice growth via positively modulating the growth-associated gene expression and endophytic microbial community

Mengchen Tian[1, 2], Zihao Zhao[1], Qingqing Li[3], Zeyu Cai[1, 2], Weili Jia[4], Xinxin Xu[1, 2], Anqi Liang[1, 2], Shuai Wang[1, 2], Jason C. White[5], Chuanxin Ma[1, 2 *], Baoshan Xing[6]

[1]Guangdong Basic Research Center of Excellence for Ecological Security and Green Development, Key Laboratory for City Cluster Environmental Safety and Green Development of the Ministry of Education, School of Ecology, Environment and Resources, Guangdong University of Technology, Guangzhou 510006, China;

[2]Guangdong Provincial Key Laboratory of Water Quality Improvement and Ecological Restoration for Watersheds, Institute of Environmental and Ecological Engineering, Guangdong University of Technology, Guangzhou 510006, China;

[3]Faculty of Arts and Sciences, Beijing Normal University, Zhuhai 519087, China;

[4]SCNU Environmental Research Institute, Guangdong Provincial Key Laboratory of Chemical Pollution and Environmental Safety & MOE Key Laboratory of Theoretical Chemistry of Environment, School of Environment, South China Normal University, Guangzhou 510006, China;

[5]The Connecticut Agricultural Experiment Station, New Haven, Connecticut 06511, United States;

[6]Stockbridge School of Agriculture, University of Massachusetts, Amherst, Massachusetts 01003, United States.

Corresponding author: chuanxin.ma@gdut.edu.cn

Number of Pages: 30

Number of Figures: 22

Text S1. nHA characterization

The TEM images of four types of nHA are shown in Figure S1A−D; all nHAs exhibit rod-like structures. The element distribution of P and Ca was further confirmed by EDS[1]. The FTIR spectra of different nHA products are shown in Figure S1E. The nHA sample contains OH^- and $PO4^{3-}$ groups in the FTIR spectrum and similar spectra were observed in 1% Cu-nHA and 10% Cu-nHA. The $PO4^{3-}$ group behaves as a well-defined doublet of v4 vibrational at wavenumbers around 565 and 600 cm^{-1}. Crystallographic analysis of different nHAs was performed by XRD, and the resulting graphs were compared with those of the standard XRD data (JCPDS No. 01-072-1243) following the standard nHAP model (Figure S1F).

Text S2. nHA effects on phytohormones

In this study, comapared with the control, root exposure to 20 nm-nHA increased several growth-related hormones in tomato and rice shoots, such as IAA (indole-3-acetic acid) and BR (brassinolide). In addition, root exposure to 1% Cu-nHA increased the content of IAA in rice shoots, but decreased the content of BR by 14.8% (Figure 2B and C). The application of 20 nm-nHA and 1% Cu-nHA did not alter the homeostasis of zeatin riboside (ZR) and dihydrozeatin (DHZR) in tomato shoots and roots, although the ZR content in rice shoots decreased by 17.1% and DHZR increased by 0.38 times (Figure 2H and I). Furthermore, comapared with the control, the application of 20 nm-nHA and 1% Cu-nHA increased the jasmonic acid (JA) content in rice shoots and roots, but decreased the JA content in tomato shoots by 15.9% with 20 nm-nHA. IAA is one of the most abundant and active auxins in plants, and can promote plant vegetative growth through cell expansion, differentiation, morphogenesis and other processes[2]. Previous studies have shown that 5 μg/mL chitosan nanoparticles (CSNPs) induce the expression of auxin-related genes, accelerate the biosynthesis and transport of IAA, and increase the endogenous IAA content in the shoots and roots of treated wheat (*Triticum aestivum* L.) by 39% and 56%, respectively, compared with the control[3]. The above results showed that the application of 20 nm-nHA and 1% Cu-nHA could increase the accumulation of growth-related hormones such as IAA and BR, thereby promoting the crop growth.

Text S3. Differentially expressed genes (DEGs) and GO enrichment analysis

Root exposure to 20 nm-nHA and 1% Cu-nHA resulted in 189 and 1591 differentially expressed genes (DEGs) in the tomato roots, respectively. In rice roots, 1075 and 2641 DEGs were found with 20 nm-nHA and 1% Cu-nHA, respectively (Figure 3E and F). The shoot DEGs of tomato and rice suggest significant differences between the 20 nm-nHA and 1% Cu-nHA treatment (Figure S14E and F). The Volcano plots show that in the tomato roots, there were 1471 up- and 763 down-regulated genes in the 20 nm-nHA treatment, and 1552 up- and 1402 down-regulated genes in the 1% Cu-nHA treatment; in the rice root,s 2572/2781 and 3518/3427 up/down-regulated genes were evident in the 20 nm-nHA and 1% Cu-nHA treatment, respectively (Figure S11). Overall, different nHA resulted in more DEGs in rice than in tomato.

Gene Ontology (GO) was used to divide all identified DEGs into three main categories (Figure S12 and S13). Both 20 nm-nHA and 1% Cu-nHA up-regulated the expression of photosynthesis-related genes in the tomato shoots and the expression of cellular glucan and glucan metabolism-associated genes in the tomato roots. Additionally, 20 nm-nHA also upregulates the expression of genes related to the glycolytic process of the tomato shoots, which is a major metabolic pathway and plays an significant role in plant development and stress response[4]. Importantly, the addition of both types of nHA did not up-regulate these GO terms in rice. Based on the reference pathway in the KEGG database, the shoot and root DEGs of tomato and rice were further annotated (Figure 3A-D and S14A-D). These DEGs in the libraries of the tomato root treated with 20 nm-nHA and 1% Cu-nHA were assigned to 93 and 113 KEGG pathways, respectively, and 109 and 117 in the tomato shoot, respectively. The DEGs in libraries of the rice root treated with 20 nm-nHA and 1% Cu-nHA were assigned to 85 and 109 KEGG pathways, respectively, and 33 and 113 in the rice shoot, respectively. Plant hormone signal transduction pathways were significantly enriched in the tomato and rice roots with 20 nm-nHA and 1% Cu-nHA. Different nHA treatments in the tomato roots impacted a number of plant hormone signal transduction pathways, linoleic acid and α-linoleic acid metabolism pathways and zeatin biosynthesis (Figure 3A and B), while different nHA treatments in the rice roots impacted plant hormone signal transduction pathways, photosynthesis pathways, amino acid metabolism, starch and sucrose metabolism pathways (Figure 4C and D).

Method S1. Plant nutrient and pigment content

Metabolite (sugars, soluble protein, amino acids) of the plant (tomato or rice) samples (shoot or root) extraction 181 were performed as described by 3,5-dinitro salicylic acid method, Bradford method, and photometric ninhydrin method.

Reducing sugar content Briefly, 0.5 g tissue were added into the centrifuge tube containing 10 mL DI water. The mixture was heated at 75°C for 30 minutes, and then add another 10 ml of water. The mixture was centrifuged at 12000 g for 5min, then 1mL of reducing sugar extract and 1mL of 3,5-dinitrosalicylic acid (DNS) were added to a 25 mL colorimetric tube, and heated in boiling water for 5 mins. Cooling the solution to room temperature in an ice bath, and finally add 25 ml of DI water to the test tube, and the absorbance was measured at 540 nm.

Soluble protein One g tissues were mixed with 5 mL PBS buffer solution (50 mM, pH7.0), and the mixture was centrifuged at 13500 *xg* for 10 mins. Mix 1 mL of supernatant with 5 mL of Coomassie brilliant blue G-250 reagent for 20 mins. The absorbance was measured at 595 nm to calculate soluble protein content.

Amino acids Briefly, accurately weigh 1 g tissue into a beaker. Add 5 mL of 10% acetic acid solution and mix thoroughly. Transfer the resulting mixture to a 100 mL volumetric flask, wash with deionized water to a constant volume. The mixture was heated at 90 °C in a water bath until the color became stable. The absorbance was measured at 595 nm to calculate amino acid content.

Chlorophyll content: The chlorophyll content of leaves is closely related to photosynthetic potential[5]. The leaves of the plants were cut into small pieces and 100 mg were placed into a centrifuge tube containing 10 mL 95 % (v/v) ethanol. Following a 3-day extraction period in the dark, the absorbance of the supernatant was measured at 665 nm, 649 nm, and 470 nm using a UV–vis spectrophotometer (UV-5500, Shanghai Metash Instruments Co., Ltd). The content of total chlorophyll and carotenoids was calculated using the following formula:

$Chla = 13.36 \times A_{665} - 5.19 \times A_{649;}$

$Chlb = 27.43 \times A_{649} - 8.12 \times A_{665};$

Total chlorophyll = Chla + Chlb;

$Carotenoids = (1000 \times A_{470} - 2.13 \times Chla - 97.64 \times Chlb)/209.$

Phytohormone: The contents of nine phytohormones (auxin, gibberellin A3, gibberellin A4, abscisic acid, zeatin, dihydrozeatin, brassinosteroids, jasmonic acid, and indole-3-acetic acid) were determined using commercial ELISA kits[6].

Method S2. Chlorophyll fluorescence kinetic imaging

After 30 minutes of initial dark acclimation to stabilize the photosynthetic organs in isolated leaves, minimal fluorescence (F_0) was measured, and then maximal fluorescence (Fm) was measured with a saturating flash of light (1 s of 4000 μmol photons m^{-2} s^{-1}). According to Maxwell and Johnson, the photochemical quantum yield (ΦPSII), the maximum quantum efficiency of PSII, and the non-photochemical quenching (NPQ) parameters were calculated[7].

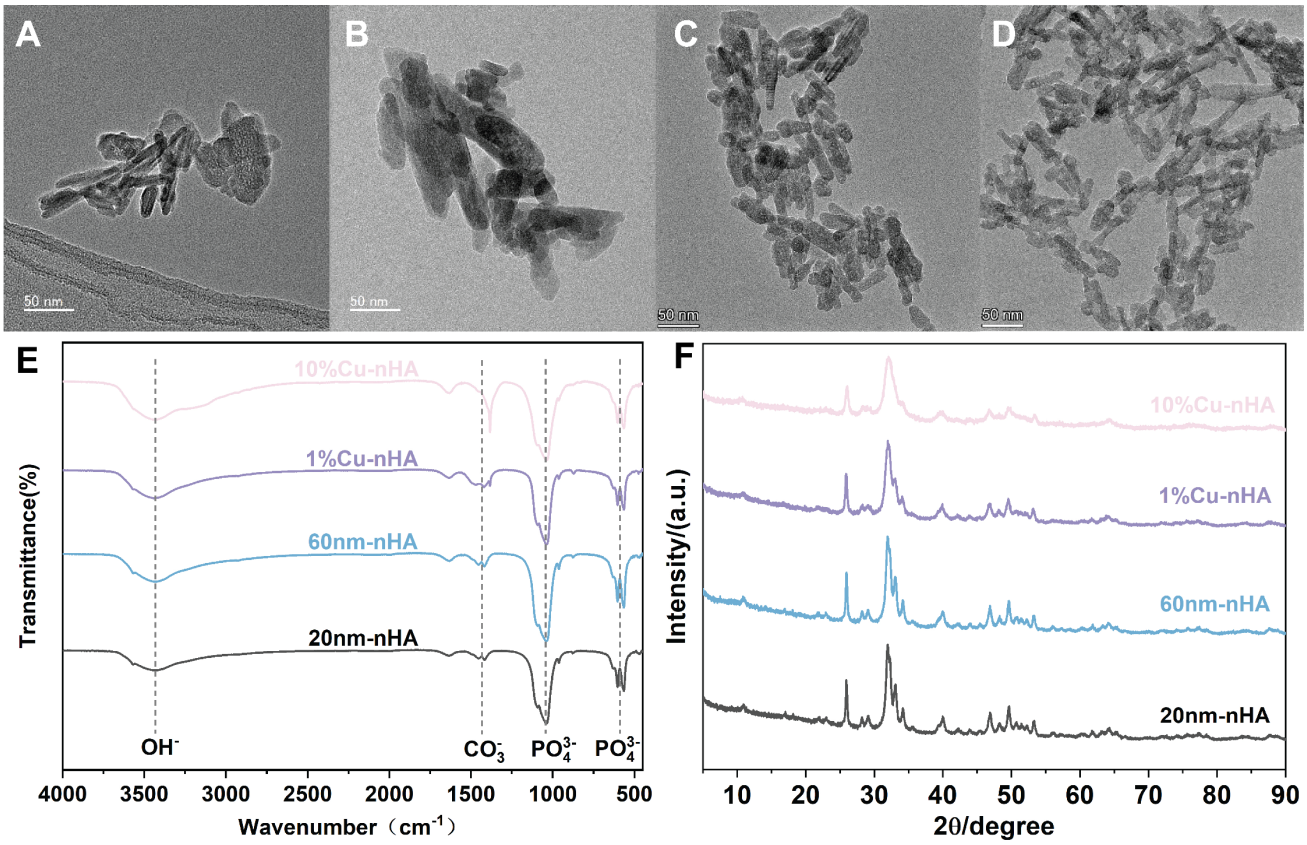

Figure S1. The characterization of 20 nm-nHA, 60 nm-nHA, 1 % Cu-nHA and 10% Cu-nHA. (A) TEM image of 20 nm-nHA; (B) TEM image of 60 nm-nHA; (C) TEM image of 1 % Cu-nHA; (D) TEM image of 10 % Cu-nHA; (E) FTIR spectra of nHA. (F) XRD patterns of nHA.

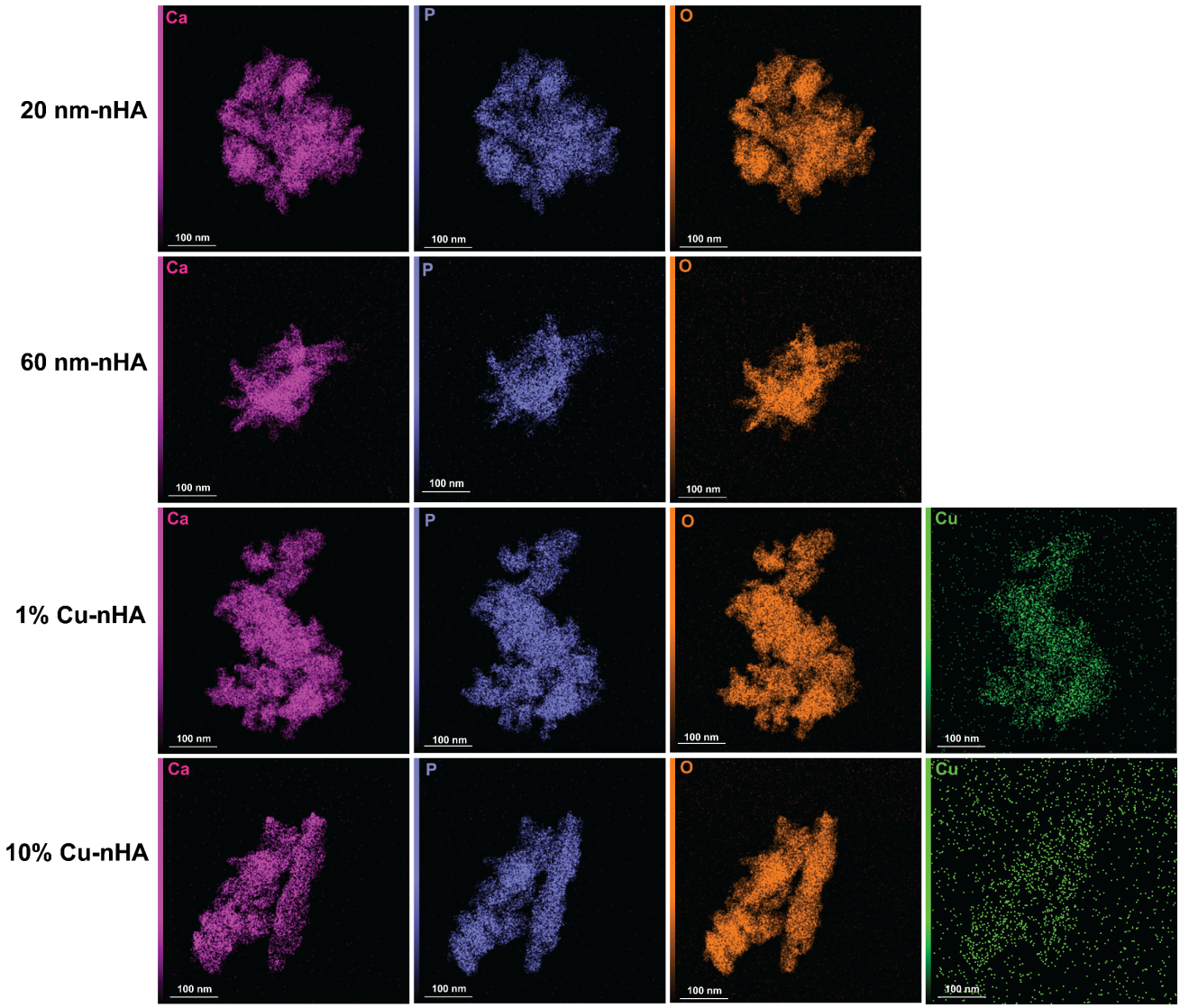

Figure S2. TEM-EDS mapping of different nHA (20 nm-nHA, 60 nm-nHA, 1 % Cu-nHA and 10% Cu-nHA).

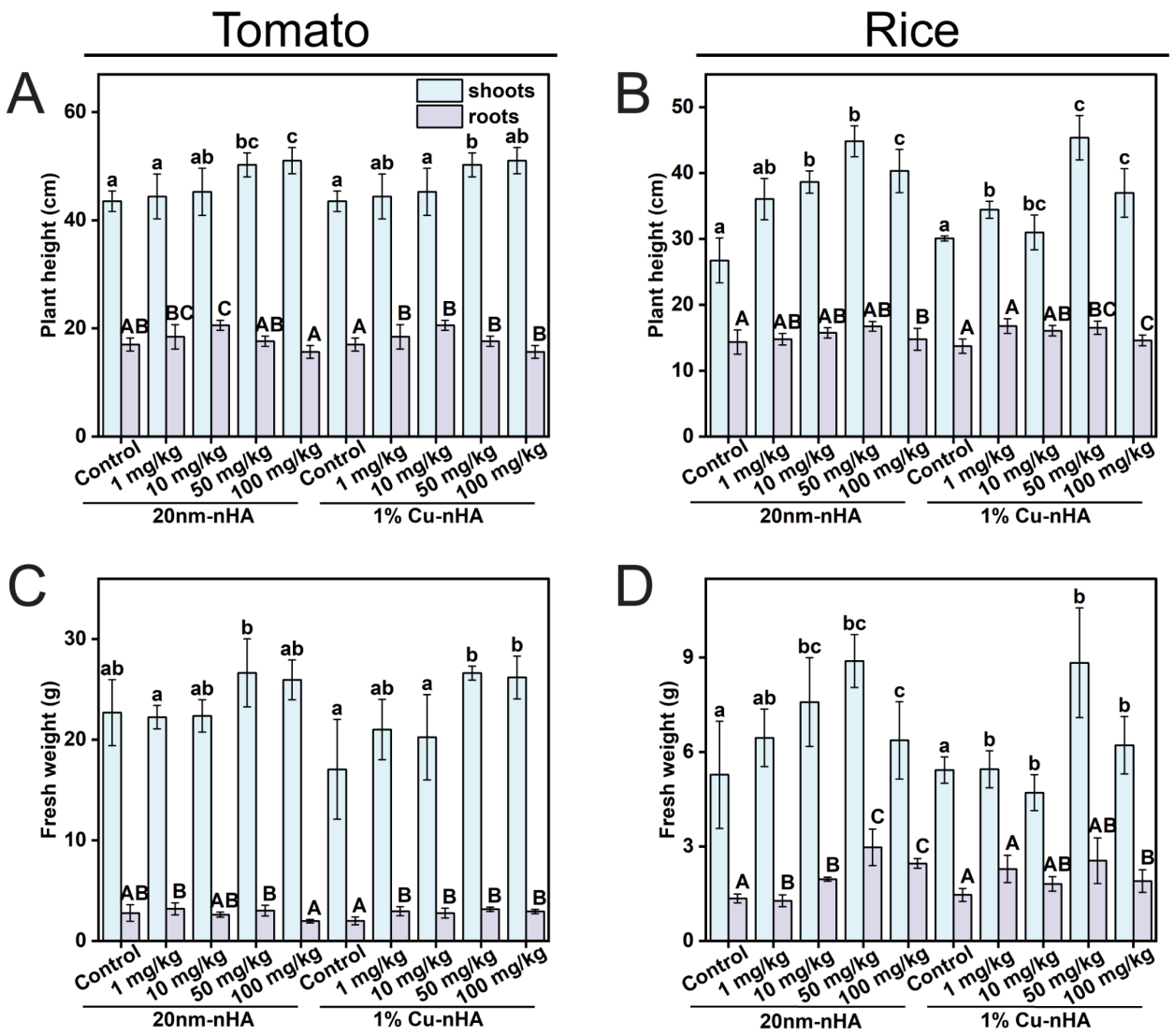

Figure S3. Physiological responses of tomato and rice seedlings upon root exposure to different types (including 20 nm-nHA and 1% Cu-nHA) and different concentrations (1 mg/kg, 10 mg/kg, 50 mg/kg, and 100 mg/kg) of nHA. (A, B) Plant height; (C, D) fresh weight. The different letters in the figure indicate significant differences ($P < 0.05$) determined by one-way ANOVA, letters in lowercase represent significant differences among shoots, while uppercase letters represent significant differences in roots.

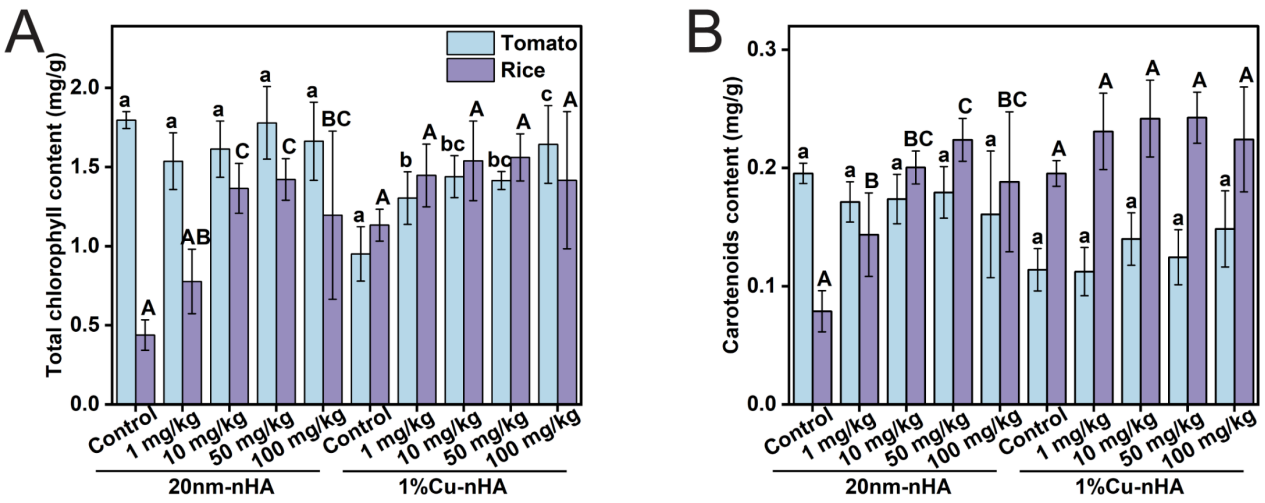

Figure S4. The content of pigments in the shoots of tomato and rice seedlings upon root exposure to different types (including 20 nm-nHA and 1% Cu-nHA) and different concentrations (1 mg/kg, 10 mg/kg, 50 mg/kg and 100 mg/kg) of nHA. (A) Chlorophyll content; (B) carotenoid content. The different letters in the figure indicate significant differences ($P < 0.05$) determined by one-way ANOVA, letters in lowercase represent significant differences among tomatoes, while uppercase letters represent significant differences in rice.

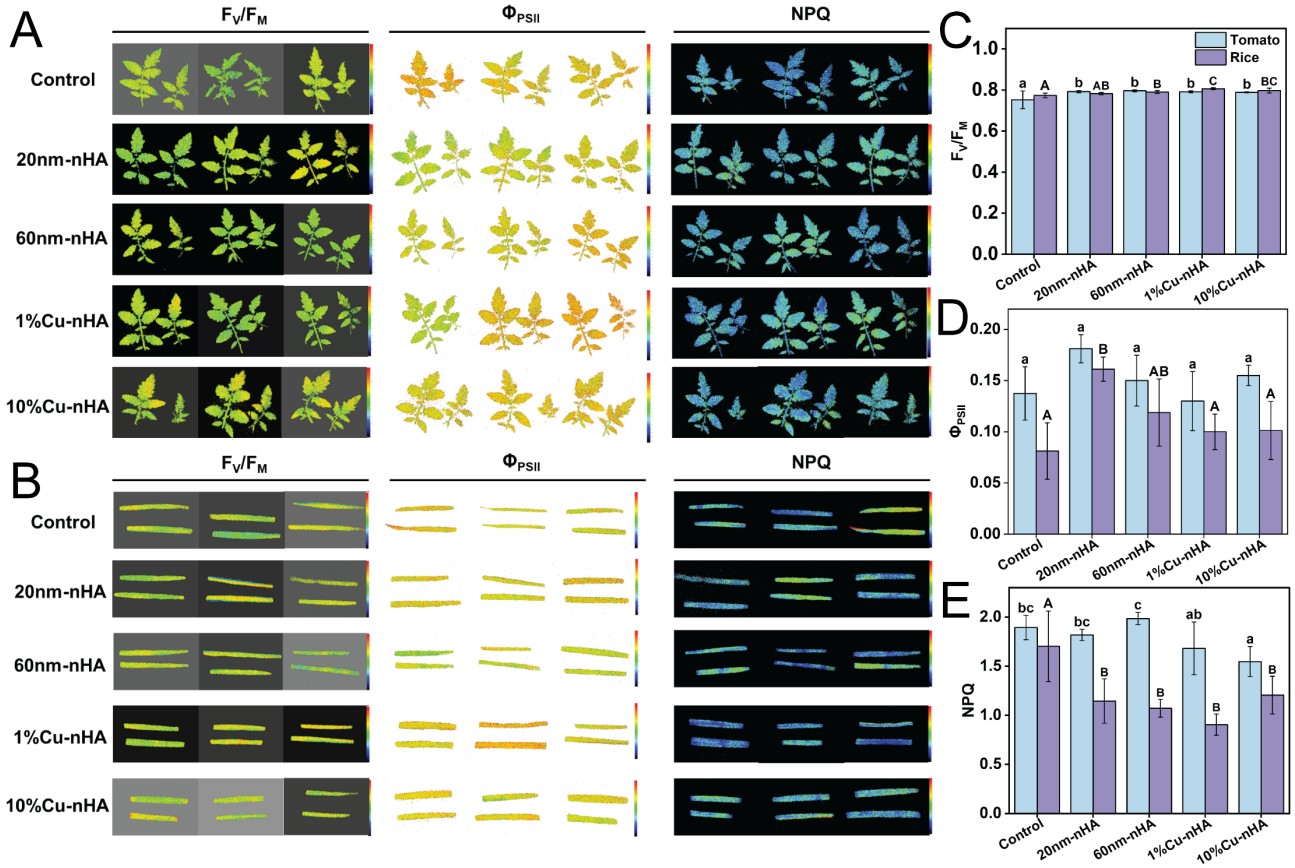

Figure S5. Changes in energy partitioning in leaves for different tomato seedlings and rice plants. (A, B) Imaging of F_V/F_M, Φ_{PSII}, and NPQ on separate leaves of tomato and rice plants; (C-E) maximum photosystem II efficiency (Fv/Fm), actual photochemical efficiency (Φ_{PSII}), and non-photochemical quenching (NPQ) in separate leaves of tomato and rice plants. The different letters in the figure indicate significant differences ($P < 0.05$) determined by one-way ANOVA, letters in lowercase represent significant differences among tomatoes, while uppercase letters represent significant differences in rice.

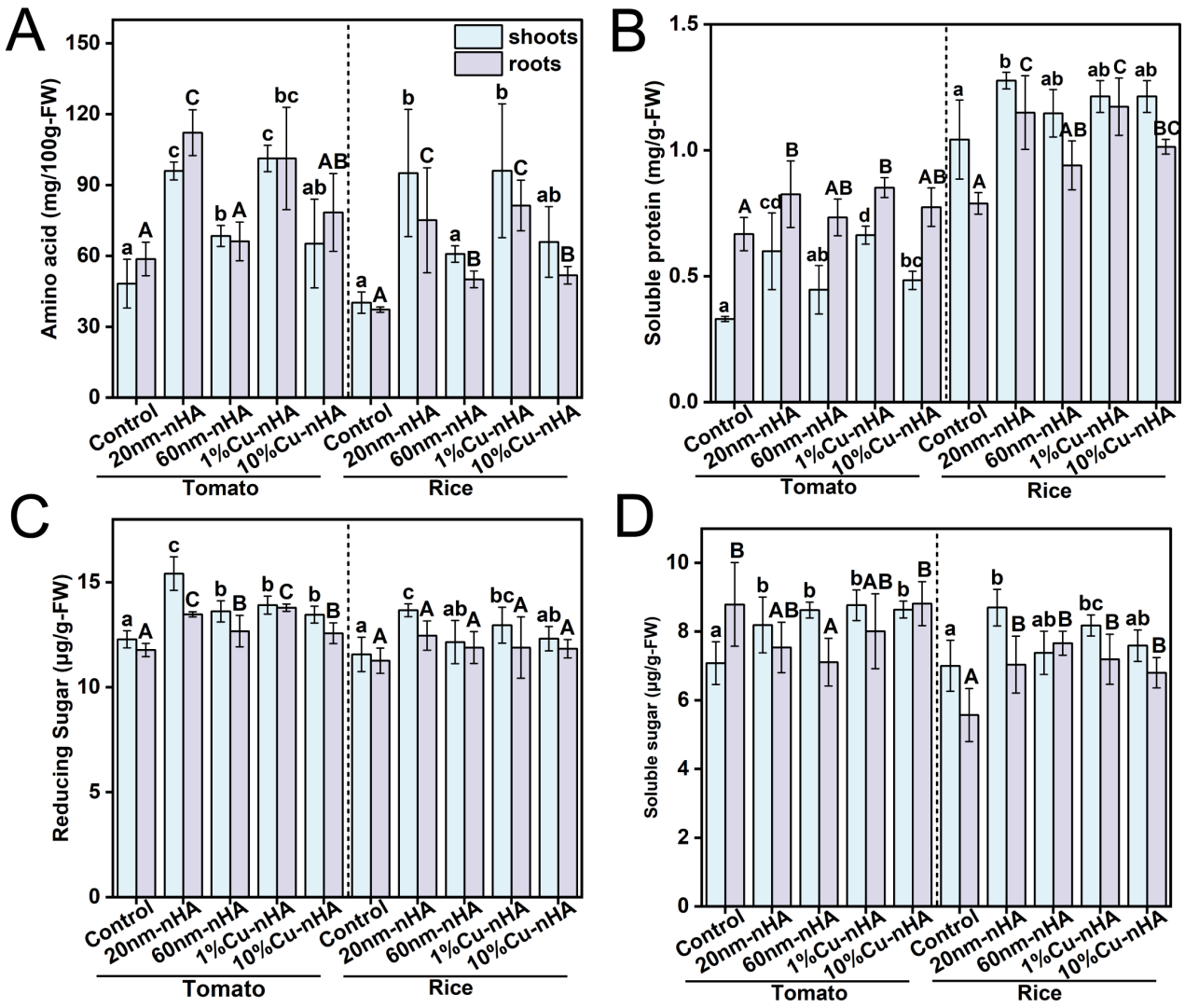

Figure S6. The contents of amino acids (A), soluble protein (B), reducing sugar (C), and soluble sugar (D) in roots and shoots of tomato and rice treated with different types of nHA via root exposure. The different letters in the figure indicate significant differences ($P < 0.05$) determined by one-way ANOVA, letters in lowercase represent significant differences among shoots, while uppercase letters represent significant differences in roots.

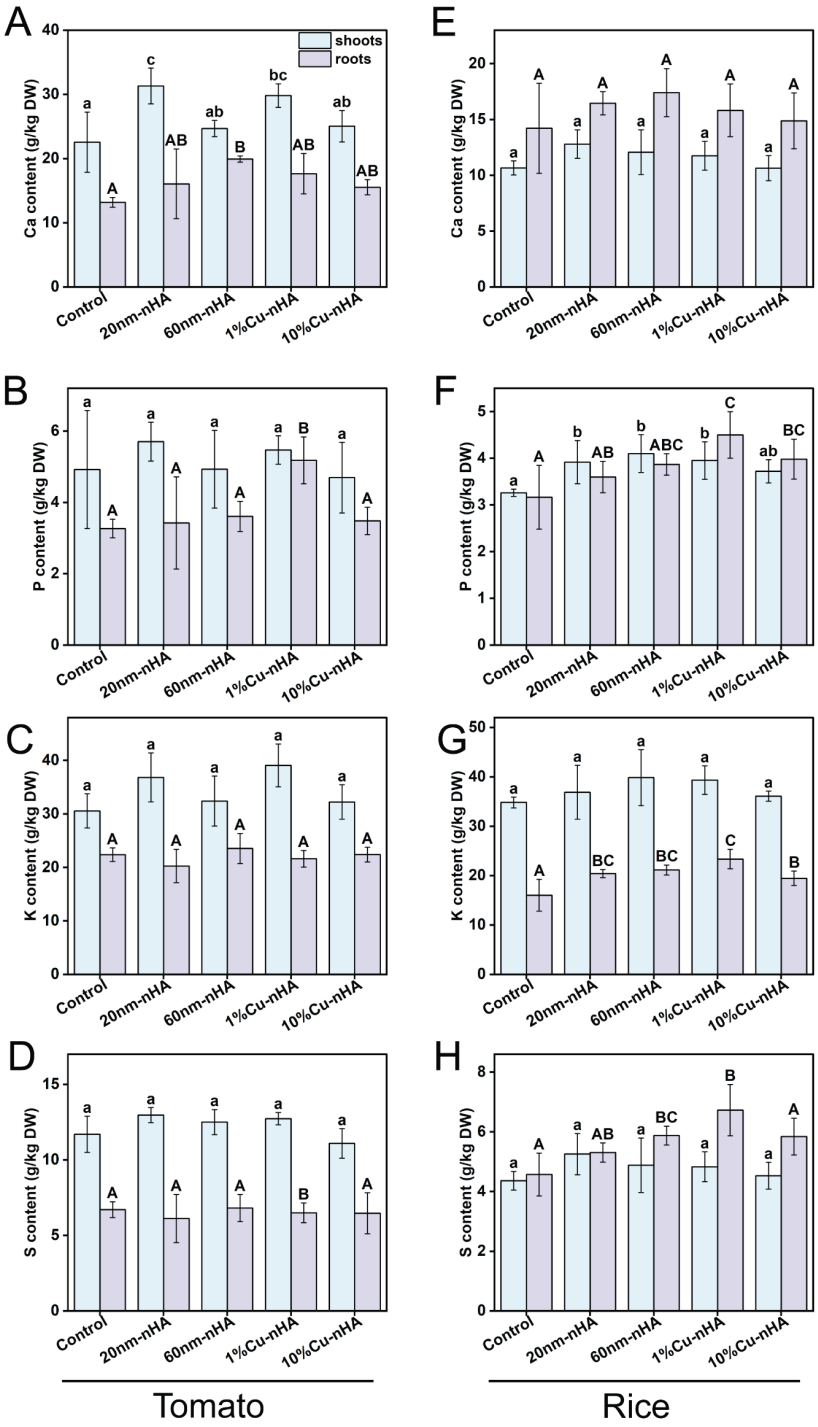

Figure S7. The micronutrient content in shoots and roots after root exposure to different types of nHA (including 20 nm-nHA, 60 nm-nHA, 1% Cu-nHA, and 10% Cu-nHA) in tomato and rice plants. (A-D) The concentration in tomato shoots and roots of macronutrients; (E-H) the concentration in rice shoots and roots of macro-nutrients. The different letters in the figure indicate significant differences ($P < 0.05$) determined by one-way ANOVA, letters in lowercase correspond to significant differences among shoots, while uppercase letters correspond to significant differences in root.

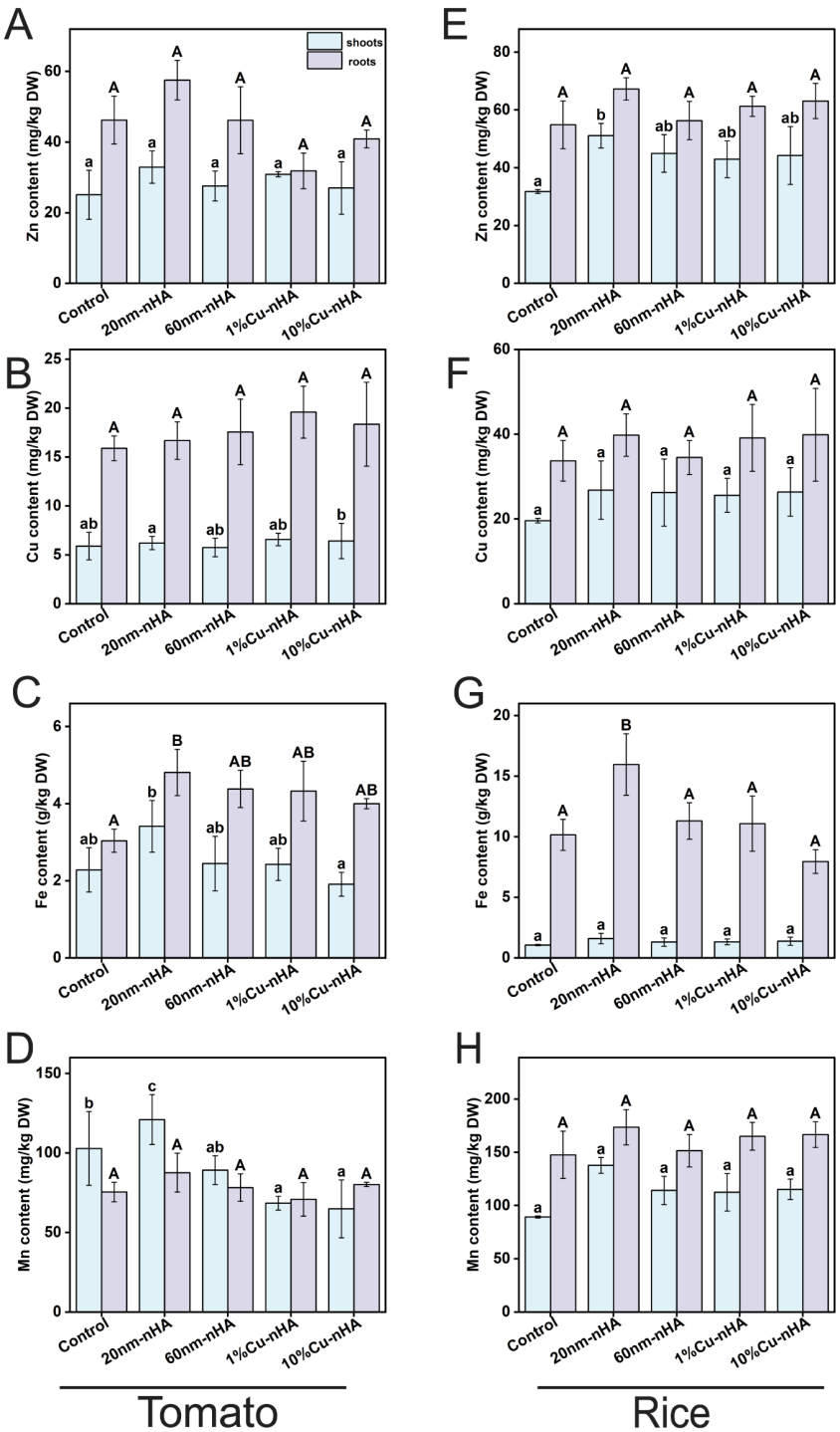

Figure S8. The micronutrient content in shoots and roots after root exposure to different types of nHA (including 20 nm-nHA, 60 nm-nHA, 1 % Cu-nHA, and 10% Cu-nHA) in tomato and rice plants. (A-D) The concentration in tomato shoots and roots of micronutrients; (E-H) the concentration in rice shoots and roots of micronutrients. The different letters in the figure indicate significant differences ($P < 0.05$) determined by one-way ANOVA, letters in lowercase correspond to significant differences among shoots, while uppercase letters correspond to significant differences in root.

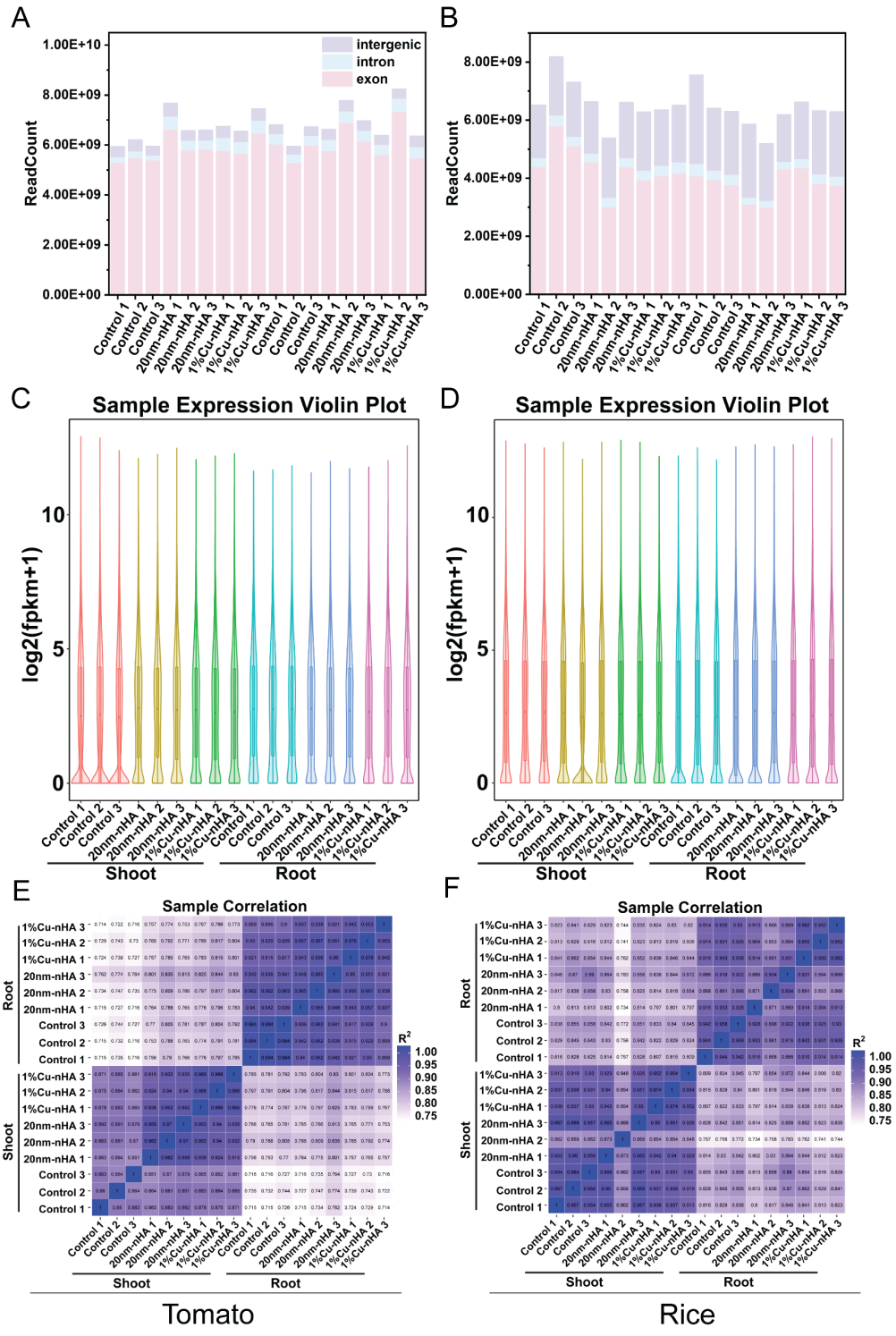

Figure S9. The quality of RNA-seq profiles. (A, B) The percentage of reads alignment region; (C, D) The Fpkm distribution of all gene expression in all samples, fragments per kilobase million. (E, F) The correlation of transcriptome between samples. The value in each cell represents the correlation coefficient.

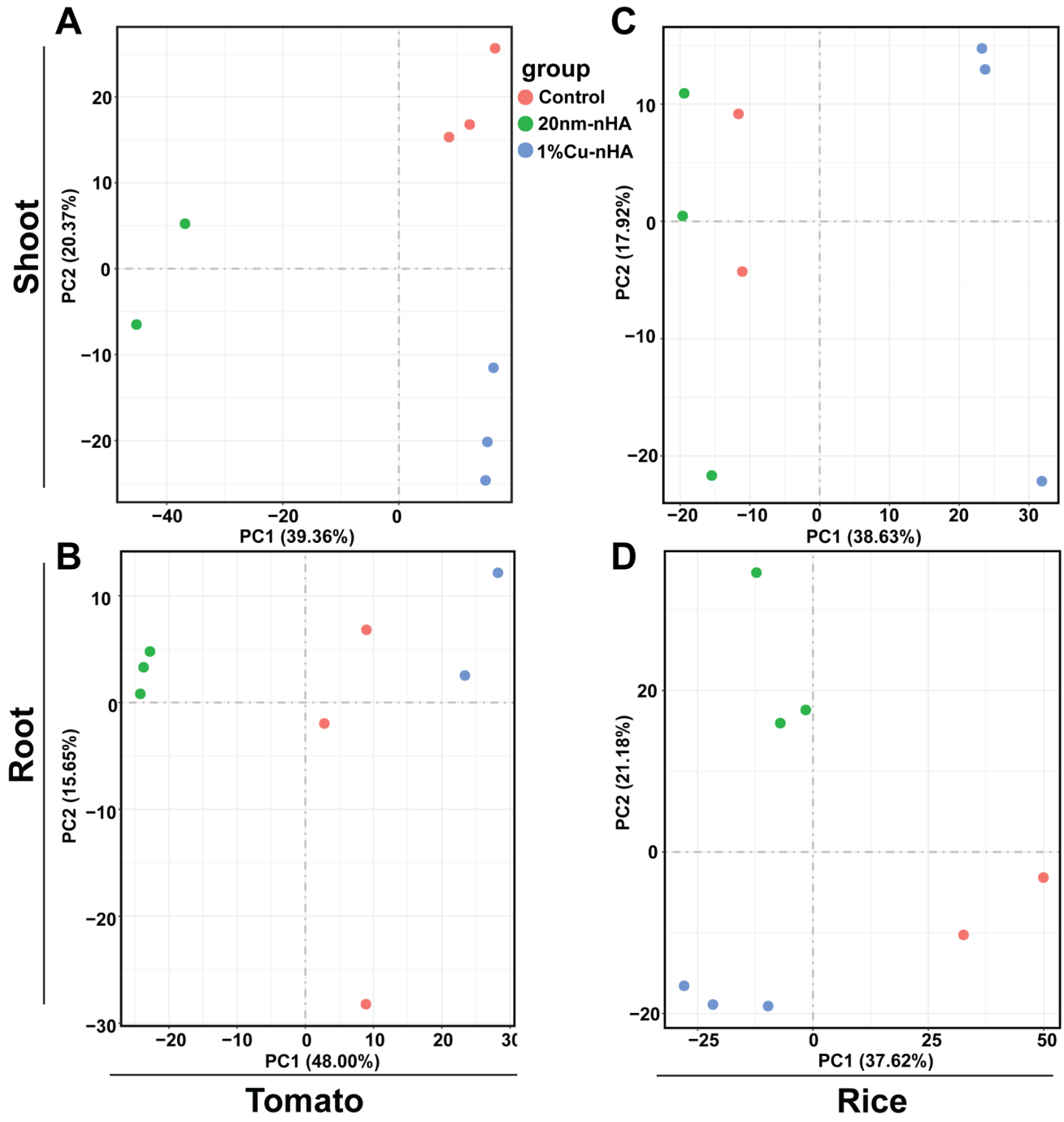

Figure S10. PCA score plot of the transcriptome in root exposure. (A) PCA score plot in tomato shoots; (B) PCA score plot in tomato roots; (C) PCA score plot in rice shoots; (D) PCA score plot in rice roots. PC1, the first principal component; PC2, the second principal component.

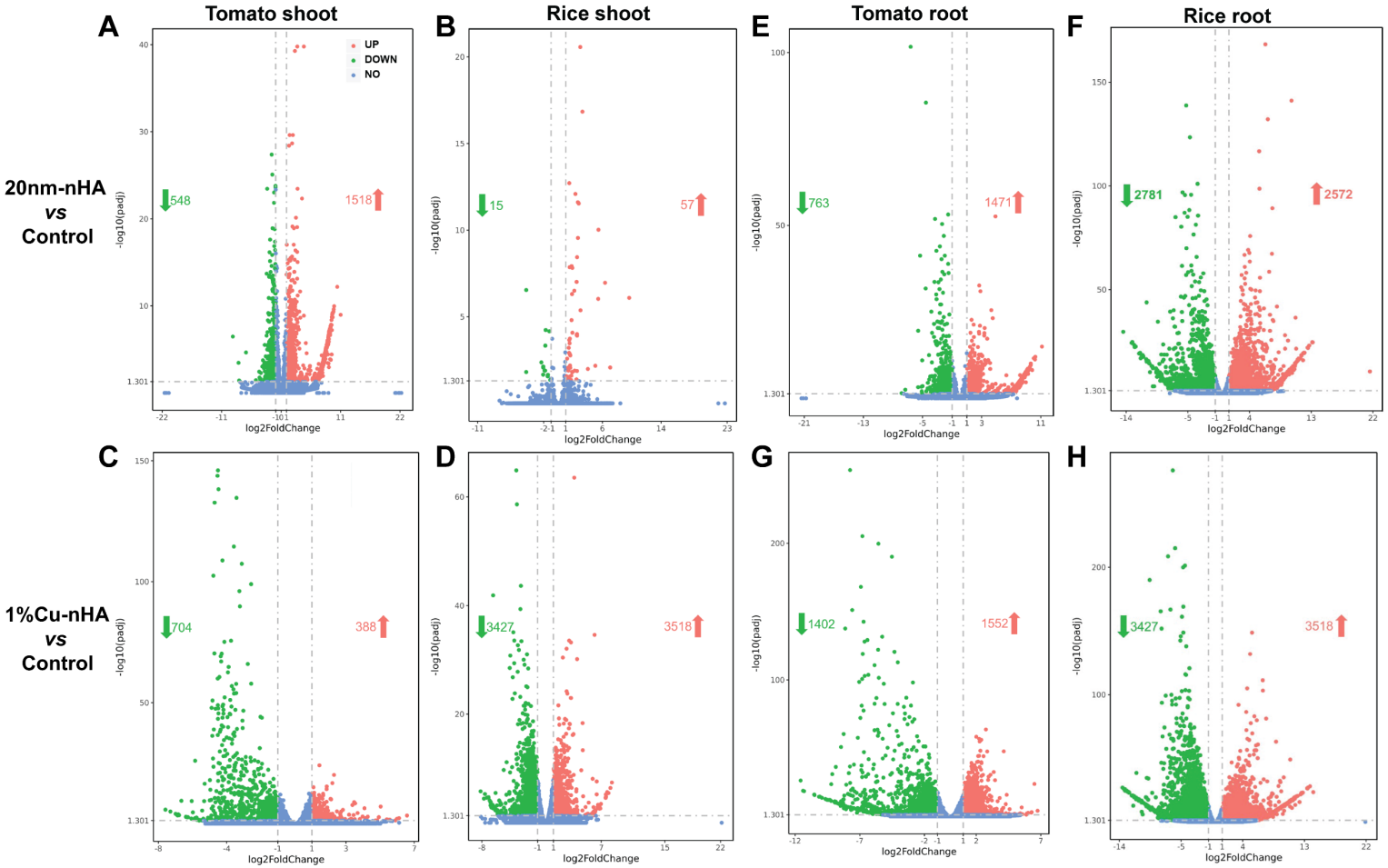

Figure S11. Volcano plot of differentially expressed genes (DEGs) in tomato and rice. (A-D) Volcano map of differentially expressed genes (DEGs) in tomato shoots and rice shoots. (E-H) Volcano map of differentially expressed genes (DEGs) in tomato roots and rice roots.

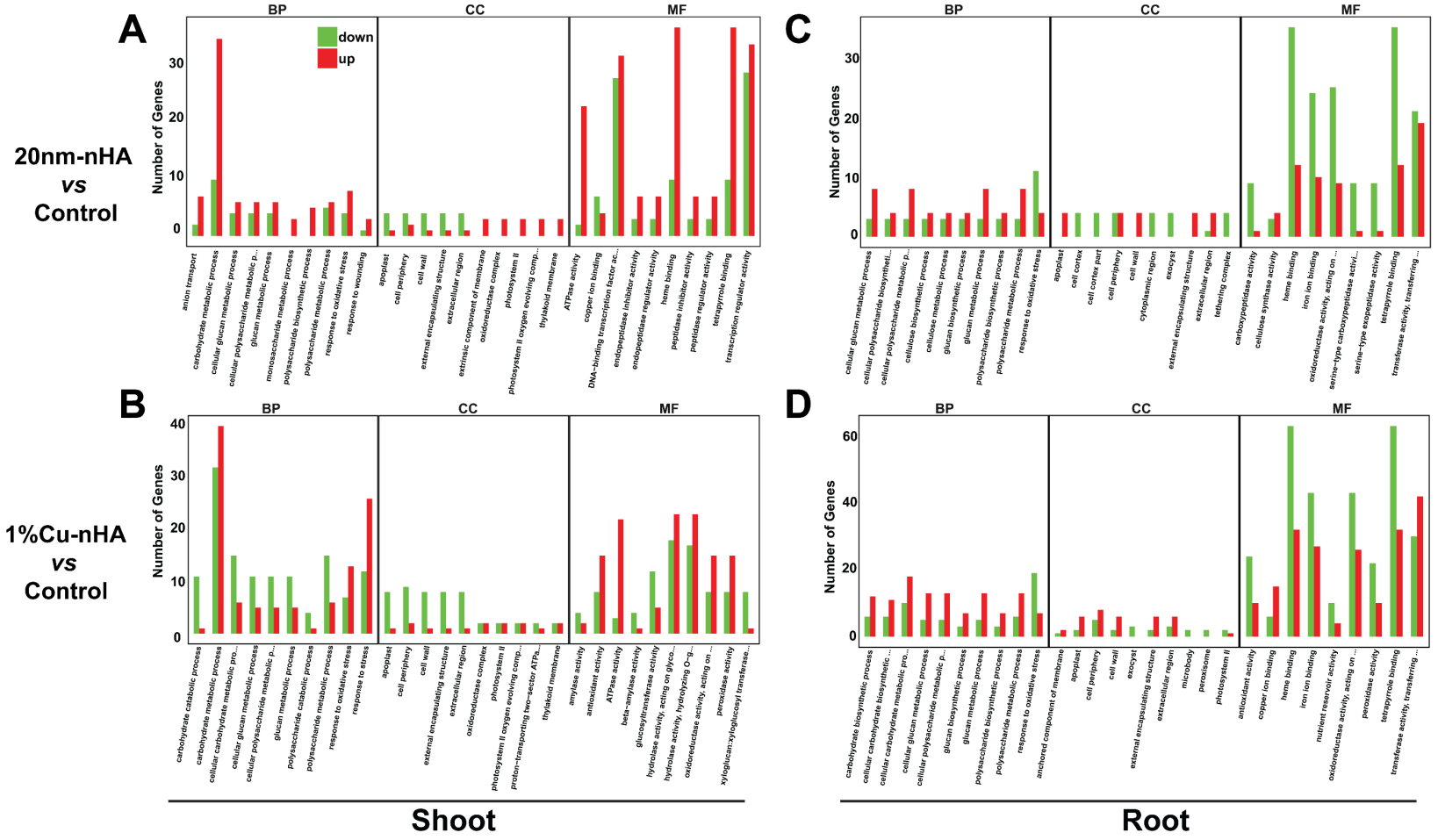

Figure S12. GO annotation of differently expressed genes. (A, B) GO annotation of differently expressed genes in tomato shoots; (C, D) GO annotation of differently expressed genes in tomato roots.

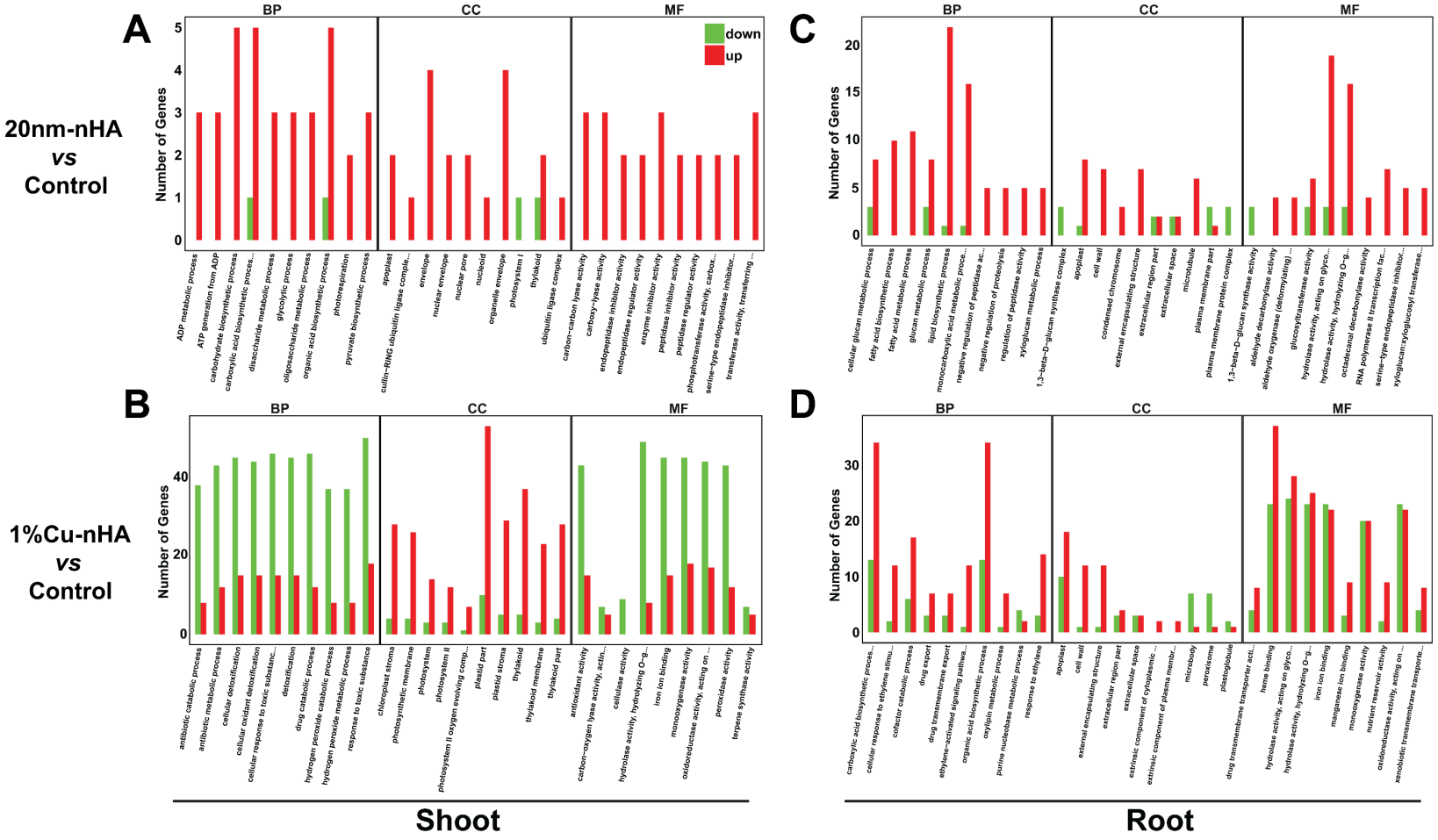

Figure S13. GO annotation of differently expressed genes. (A, B) GO annotation of differently expressed genes in rice shoots; (C, D) GO annotation of differently expressed genes in rice roots.

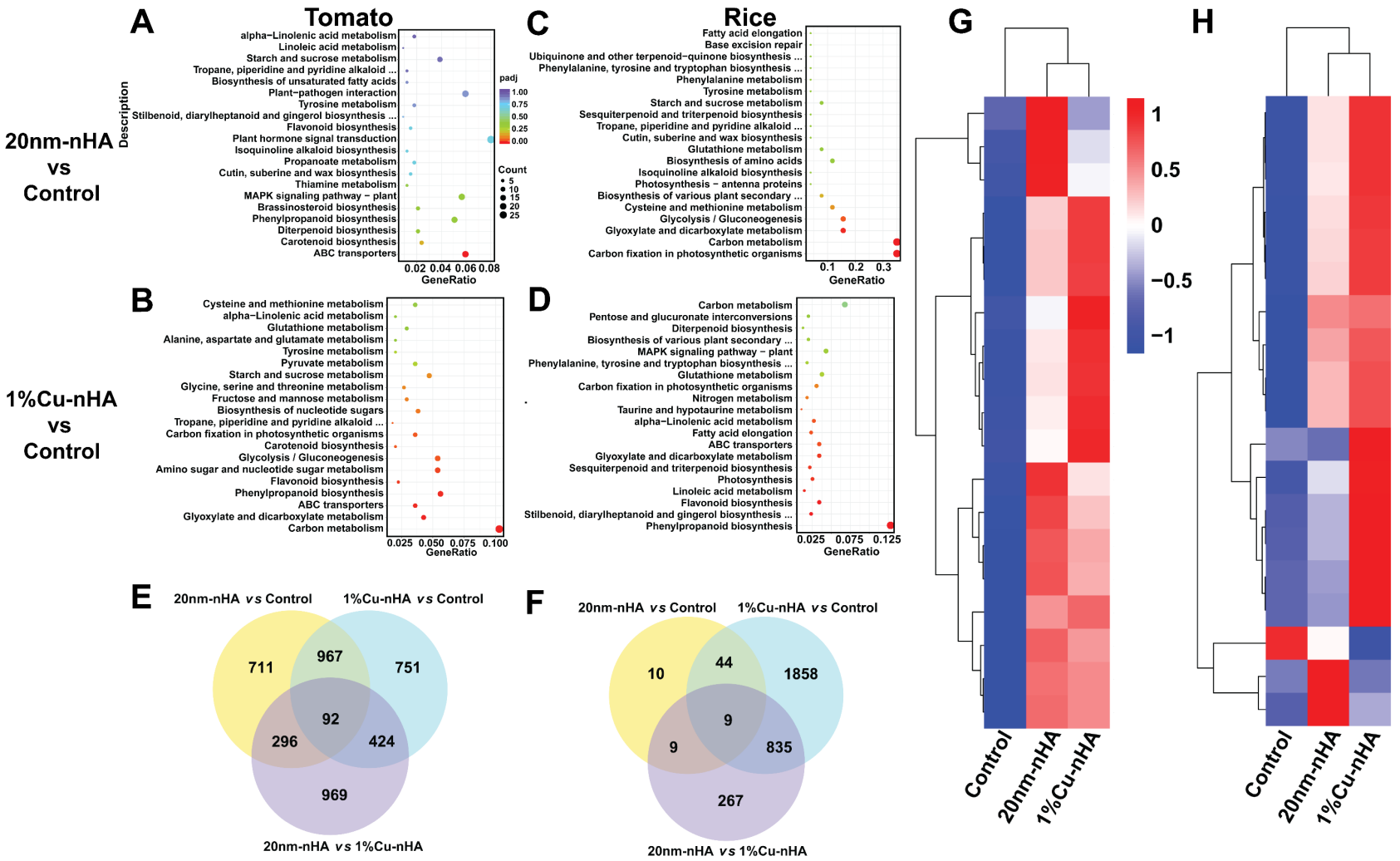

Figure S14. The transcriptome profiles of tomato shoots and rice shoots in each group. The top 20 KEGG pathways with significant enrichment of DEGs in the leaves of tomato and rice shoots (A-D) were exposed to 20 nm-nHA and 1 % Cu-nHA. (E) Venn diagram of DEGs in tomato shoots. (F) Venn diagram of DEGs in rice roots. Cluster heatmap of DEGs in tomato shoots (G) and rice shoots (H).

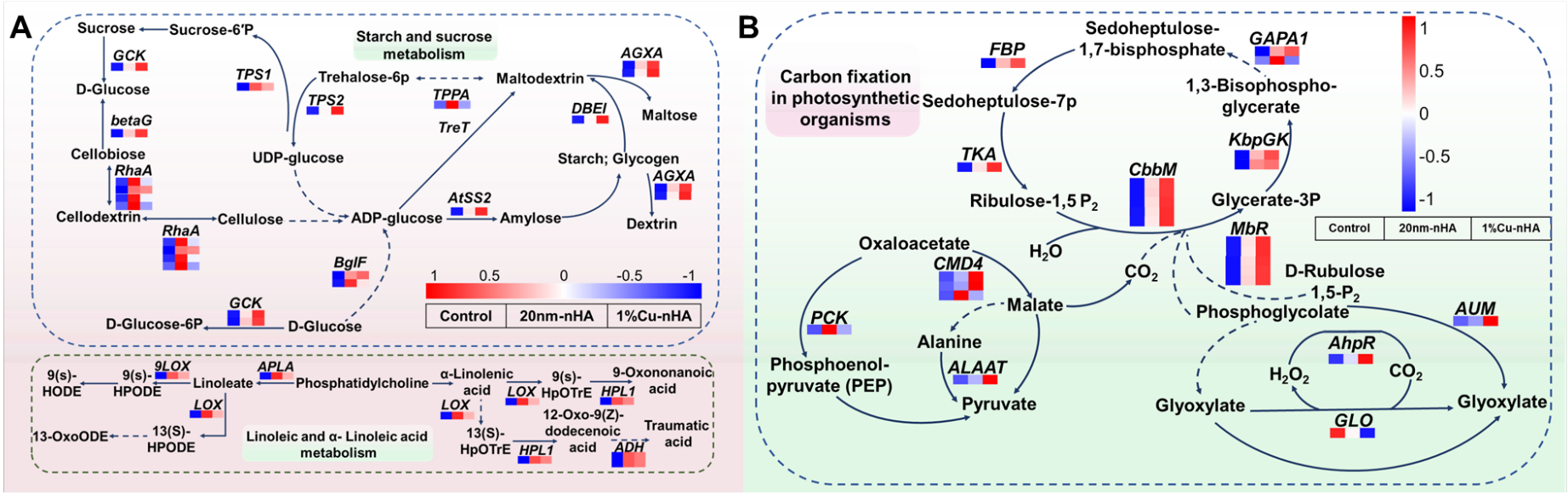

Figure S15. The KEGG pathway network of DEGs in tomato (A) and rice shoots (B) was regulated by 20nm-nHA and 1% Cu-nHA. The heatmap of the expression of DEGs was added; the log2 value of the level of gene expression shares the color key inserted below the figure.

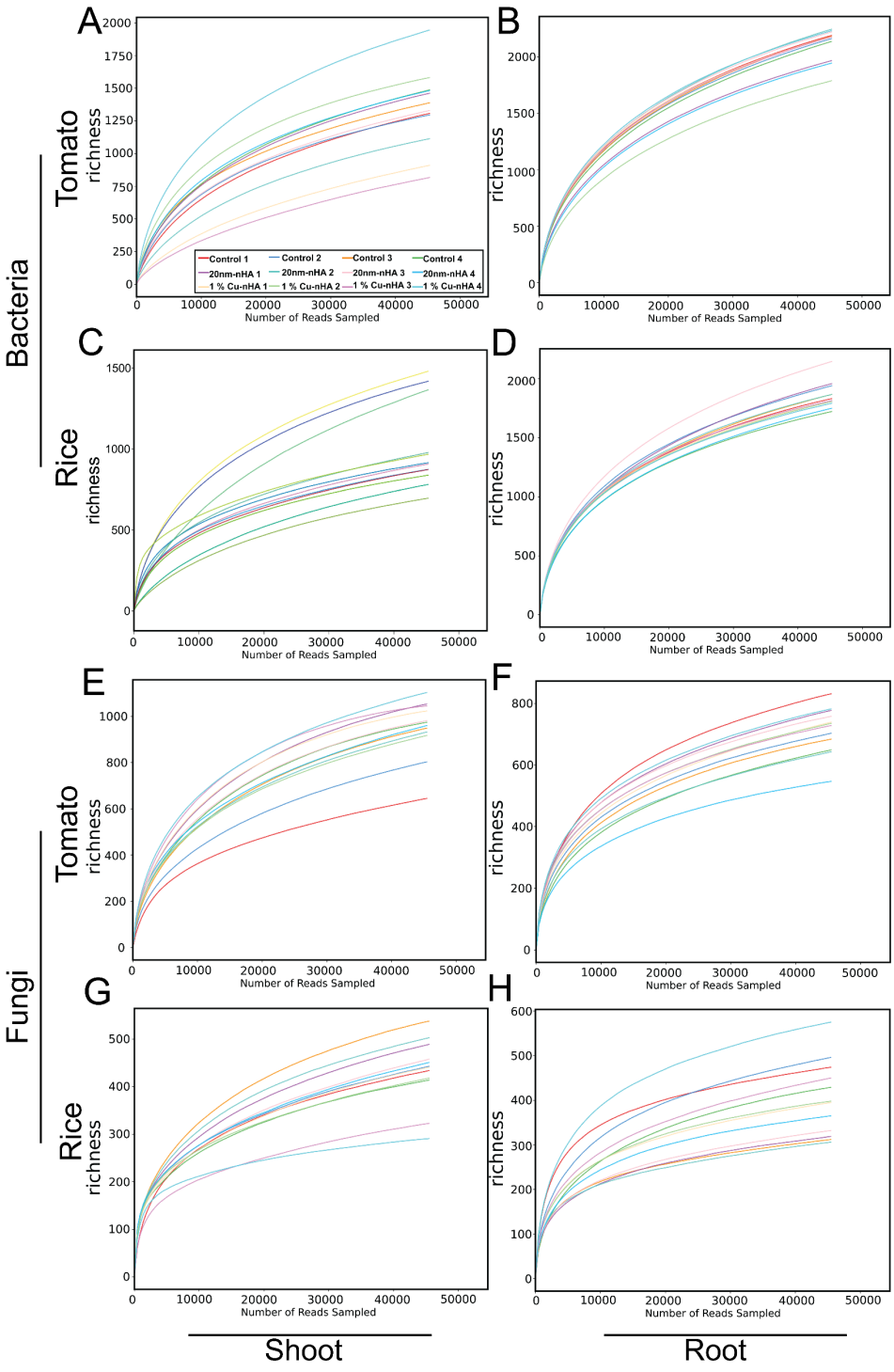

200

201 **Figure S16.** Rarefaction curves of all samples in tomato and rice across all treatments.
202 The solid lines are established by rarefaction of the measured data. (A-B) Bacterial
203 communities in tomato shoot and root; (C-D) bacterial communities in rice shoot and
204 root; (E-F) fungal communities in tomato shoot and root; (G-H) fungal communities in
205 rice shoot and root.

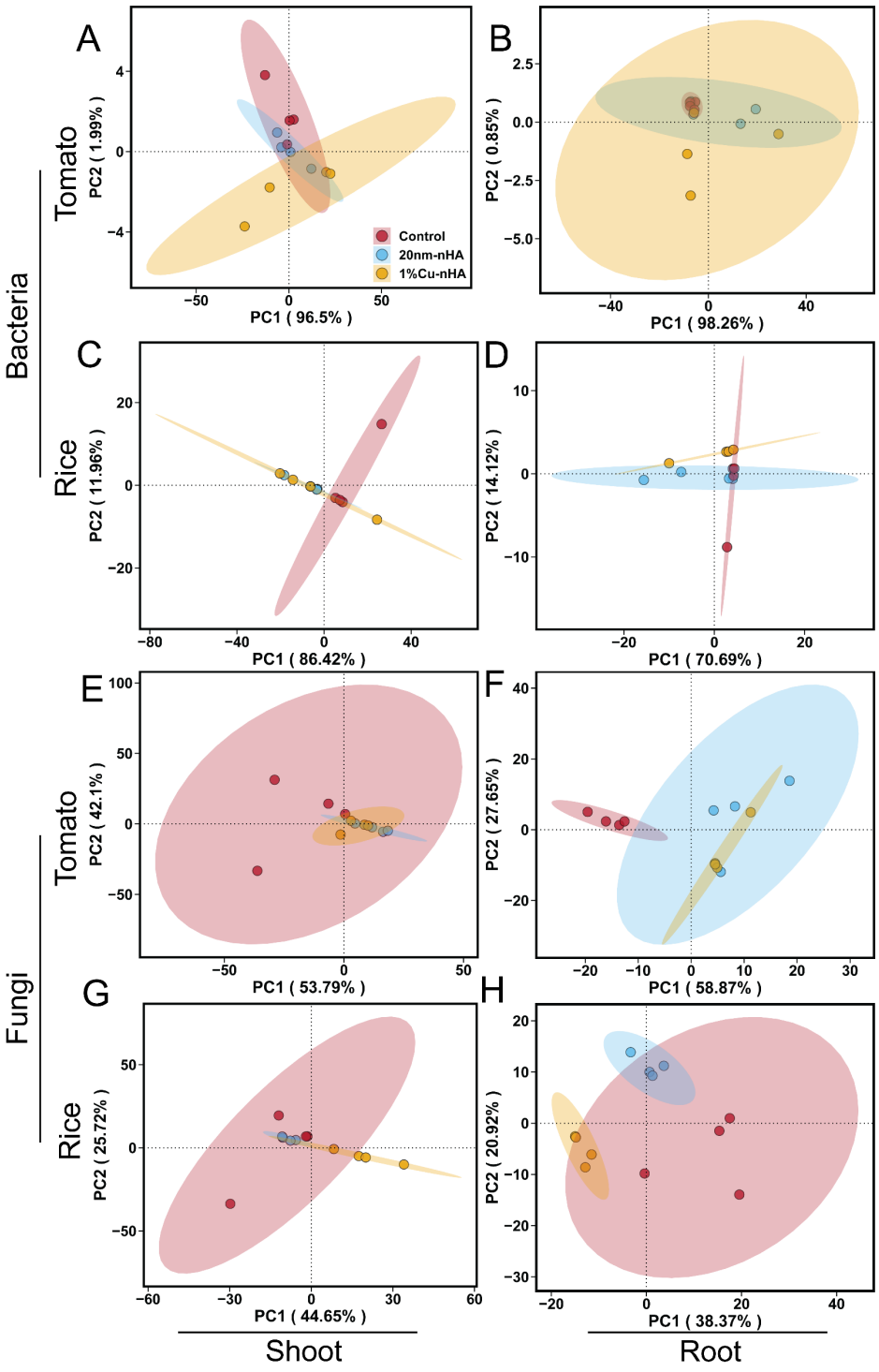

Figure S17. PCA analysis of bacterial and fungal community structure in plants treated with different nHA (20 nm-nHA and 1 % Cu-nHA). (A, B) PCA analysis of bacterial communities in tomato shoots and roots; (C, D) PCA analysis of bacterial communities in rice shoots and roots; (E, F) PCA analysis of fungal communities in tomato shoots and roots; (G, H) PCA analysis of fungal communities in rice shoots and roots.

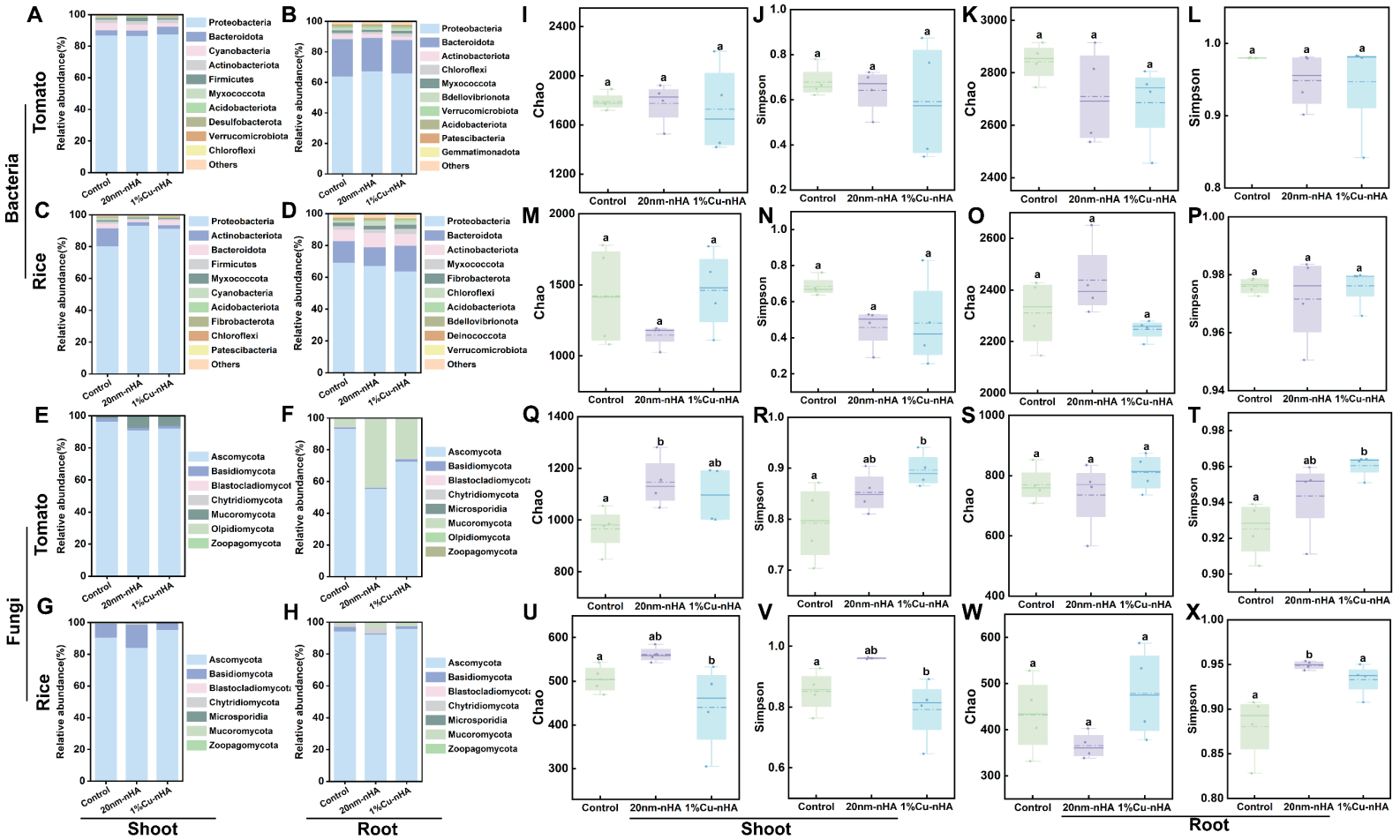

Figure S18. Relative abundances of phylum and microbial community diversity in tomato and rice treated with different nHA (20 nm-nHA and 1 % Cu-nHA).

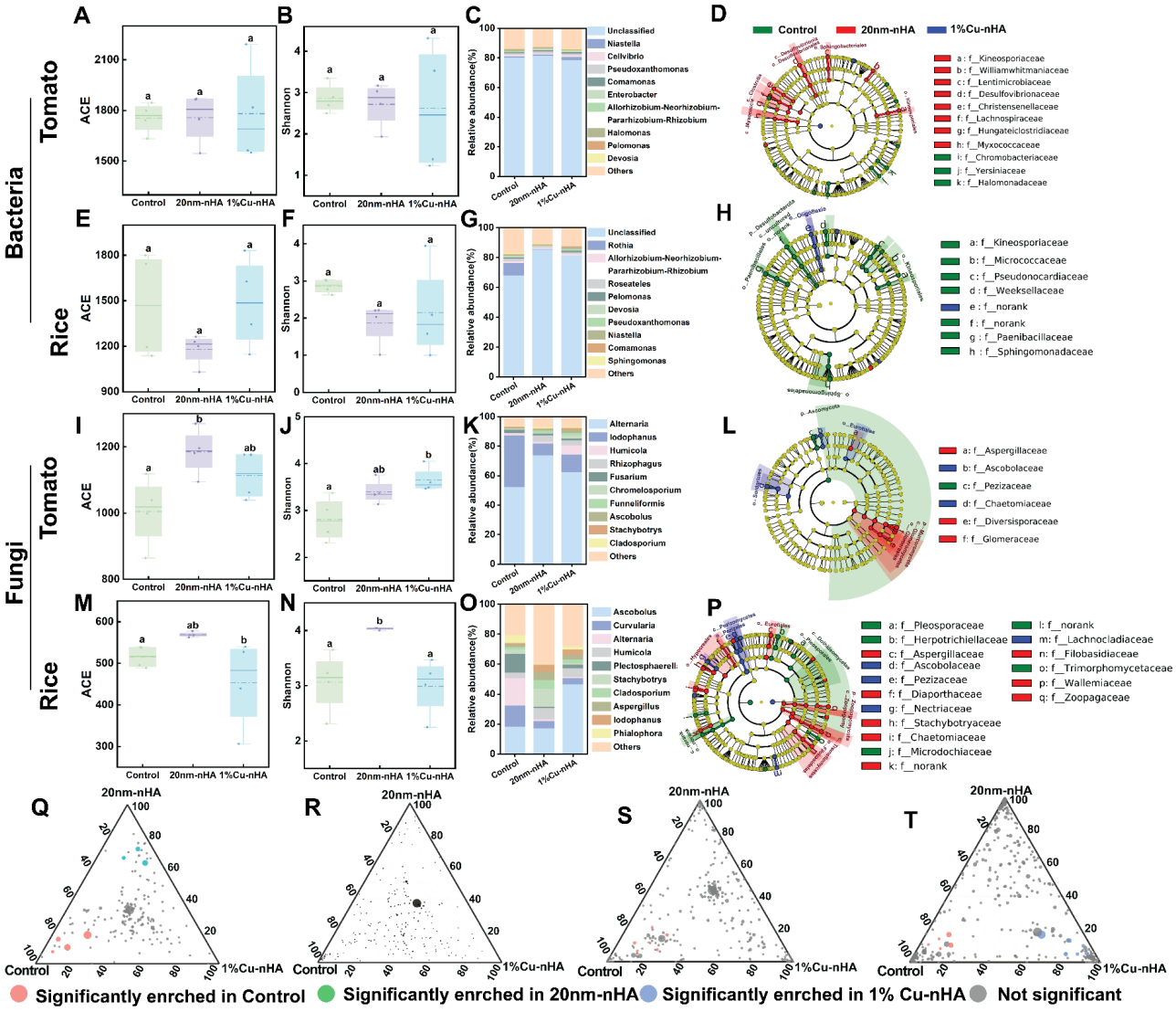

Figure S19. Community of endophytic bacteria in shoots of tomato and rice plants as affected by different nHA (20 nm-nHA and 1 % Cu-nHA). (A, B) ACE and Shannon's index of the endophytic bacterial community in tomato shoots; (C, G) the relative abundance of endophytic bacteria at the genus level in tomato and rice shoots; (D, H) cladograms of LEfSe showing bacterial indicator taxa treated with different nHA in tomato and rice shoots; (E, F) ACE and Shannon's index of the endophytic bacterial community in rice shoots; (I, J) ACE and Shannon's index of the endophytic fungal community in tomato shoots; (K, O) the relative abundance of endophytic fungus at the genus level in tomato and rice shoots; (L, P) cladograms of LEfSe showing fungal indicator taxa treated with different nHA in tomato and rice shoots; (M, N) ACE and Shannon's index of the endophytic fungal community in rice shoots; (Q−T) ternary plot of fungi from left to right describes the bacterial communities in tomato shoots, bacterial communities in rice shoots, fungal communities in tomato shoots and fungal communities in rice shoots as affected by different nHA. Each circle in the ternary plot represents an OTU detected in the data set, the circle size indicates its relative abundance.

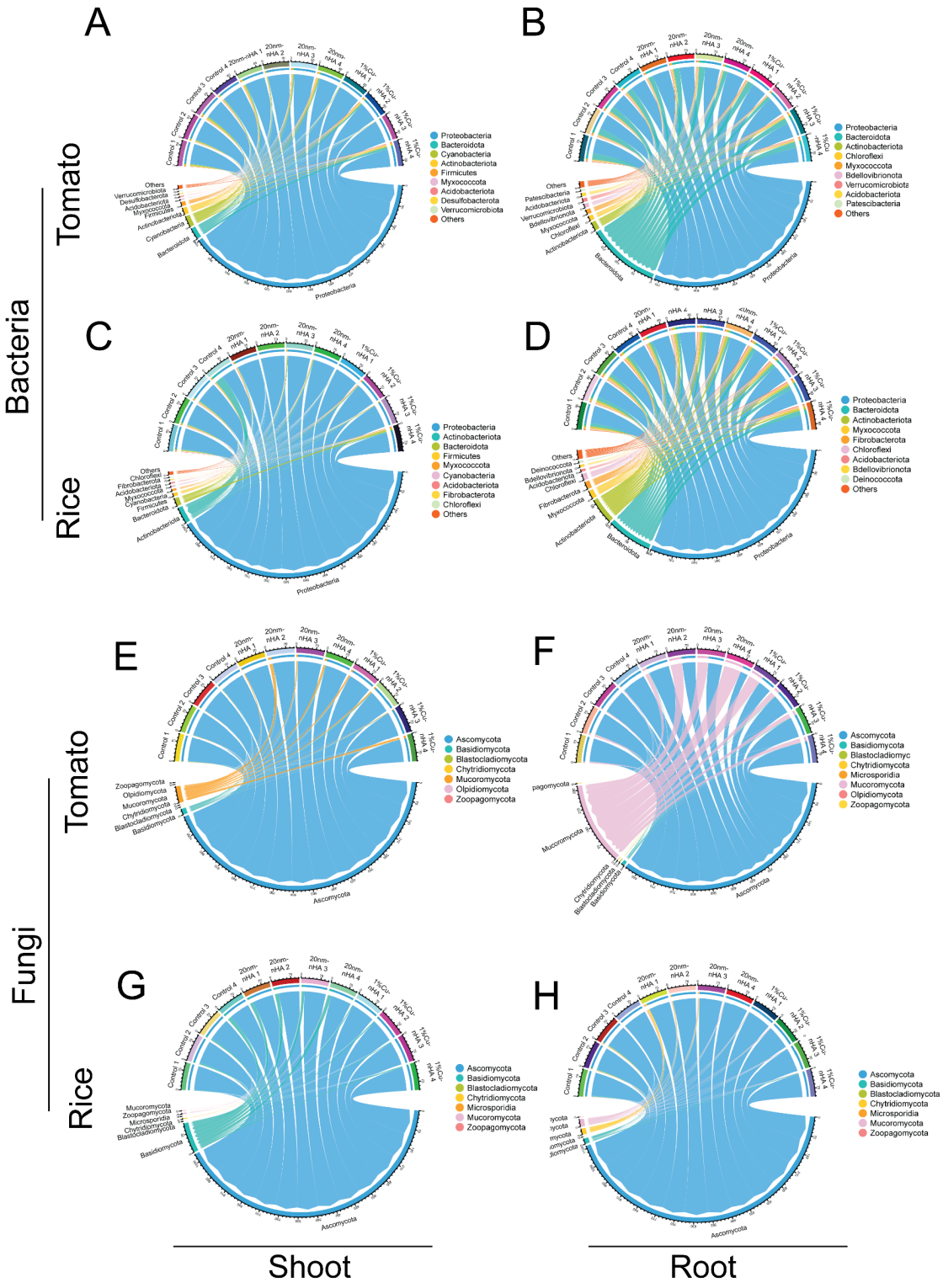

Figure S20. The composition of bacterial and fungal communities is affected by different nHA (20 nm-nHA and 1 % Cu-nHA) at the phylum level. (A, B) Bacterial communities in tomato shoots and roots; (C-D) bacterial communities in rice shoots and roots; (E-F) fungal communities in tomato shoots and roots; (G-H) fungal communities in rice shoots and roots.

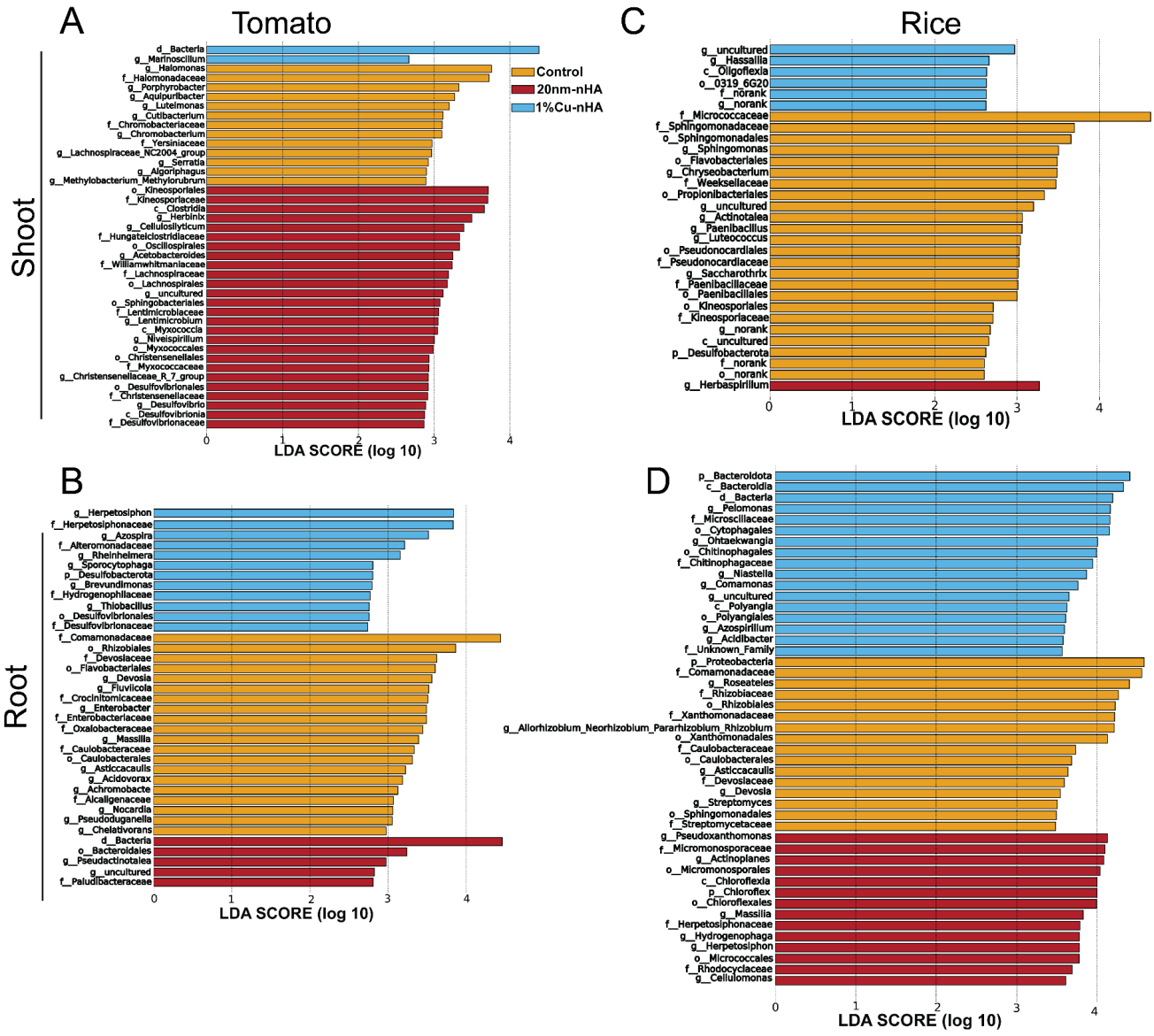

Figure S21. The LDA score plots show the endophytic bacterial community composition as affected by different nHA (20 nm-nHA and 1 % Cu-nHA). (A, B) The LDA score plots in tomato shoots and roots; (C, D) the LDA score plots in rice shoots and roots.

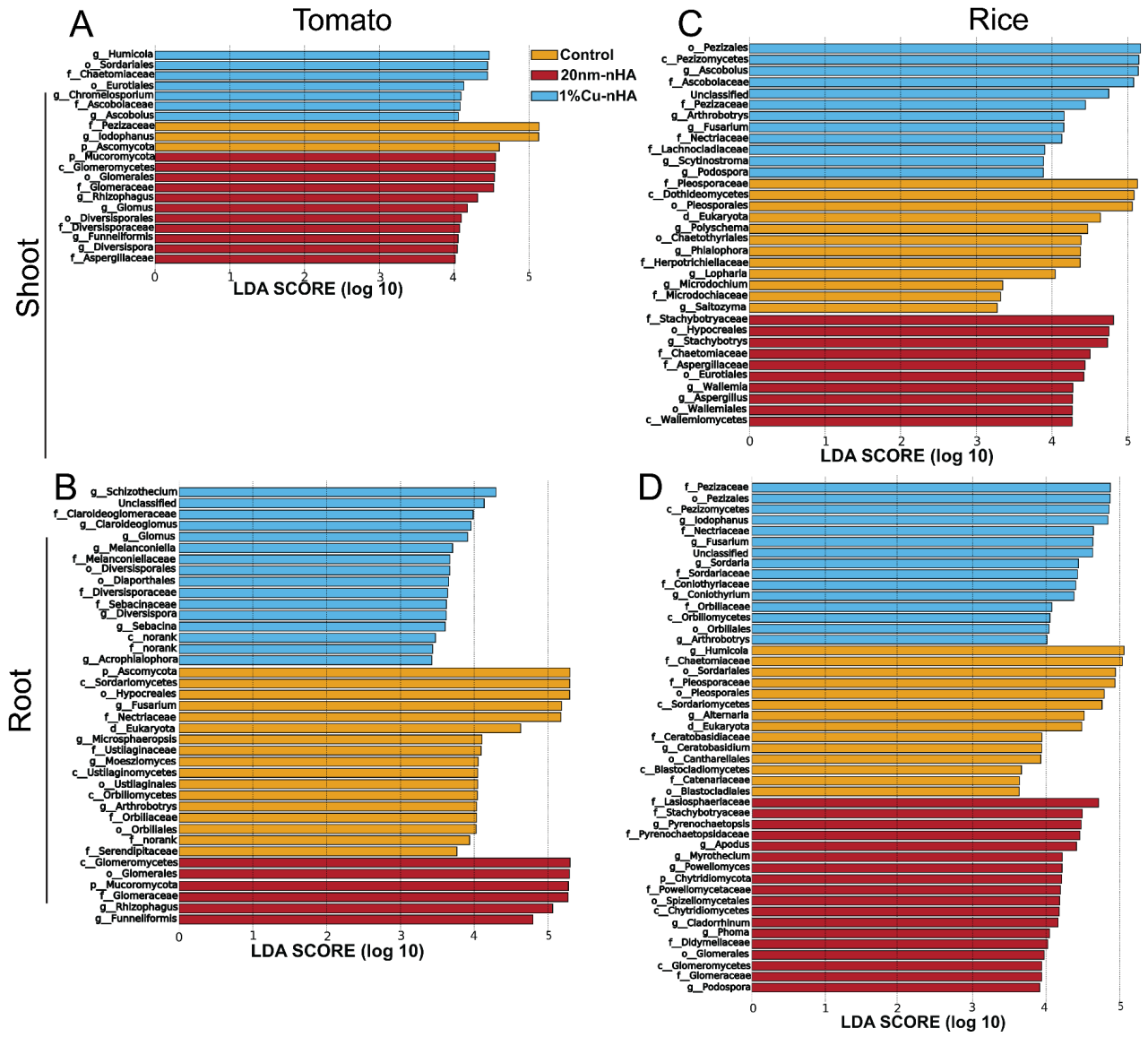

Figure S22. The LDA score plots show the endophytic fungal community composition as affected by different nHA (20 nm-nHA and 1 % Cu-nHA). (A, B) The LDA score plots in tomato shoots and roots; (C, D) the LDA score plots in rice shoots and roots.

References

1. Zhang, W.-h.; Sun, R.-b.; Xu, L.; Liang, J.-n.; Zhou, J., Assessment of bacterial communities in Cu-contaminated soil immobilized by a one-time application of micro-/nano-hydroxyapatite and phytoremediation for 3 years. *Chemosphere* **2019,** *223*, 240-249.
2. ElShamey, E. A. Z.; Hamad, H. S.; Alshallash, K. S.; Alghuthaymi, M. A.; Ghazy, M. I.; Sakran, R. M.; Selim, M. E.; ElSayed, M. A. A.; Abdelmegeed, T. M.; Okasha, S. A.; Behiry, S. I.; Boudiar, R.; Mansour, E., Growth Regulators Improve Outcrossing Rate of Diverse Rice Cytoplasmic Male Sterile Lines through Affecting Floral Traits. *Plants* **2022,** *11* (10).
3. Li, R.; He, J.; Xie, H.; Wang, W.; Bose, S. K.; Sun, Y.; Hu, J.; Yin, H., Effects of chitosan nanoparticles on seed germination and seedling growth of wheat (Triticum aestivum L.). *International Journal of Biological Macromolecules* **2019,** *126*, 91-100.
4. Givan, C. V., Evolving concepts in plant glycolysis: two centuries of progress. *Biological Reviews* **2007,** *74* (3), 277-309.
5. Lichtenthaler, H. K., [34] Chlorophylls and carotenoids: Pigments of photosynthetic biomembranes. In *Methods in Enzymology*, Academic Press: 1987; Vol. 148, pp 350-382.
6. Busoms, S.; Terés, J.; Yant, L.; Poschenrieder, C.; Salt, D. E., Adaptation to coastal soils through pleiotropic boosting of ion and stress hormone concentrations in wild Arabidopsis thaliana. *New Phytologist* **2021,** *232* (1), 208-220.
7. Maxwell, K.; Johnson, G. N., Chlorophyll fluorescence—a practical guide. *Journal of Experimental Botany* **2000,** *51* (345), 659-668.